IEEE Access
Multidisciplinary | Rapid Review | Open Access Journal

Received September 4, 2019, accepted October 7, 2019, date of publication October 16, 2019, date of current version October 29, 2019.

Digital Object Identifier 10.1109/ACCESS.2019.2947711

Multifrequency Identification and Exploitation in Lamb Wave Inspection

ZHE WANG[1], SONGLING HUANG[1], (Senior Member, IEEE), SHEN WANG[1], QING WANG[2], (Senior Member, IEEE), AND WEI ZHAO[1]

[1]State Key Laboratory of Power System, Department of Electrical Engineering, Tsinghua University, Beijing 100084, China
[2]Department of Engineering, Durham University, Durham DH1 3LE, U.K.

Corresponding author: Songling Huang (huangsling@tsinghua.edu.cn)

This work was supported in part by the National Key Research and Development Program of China under Grant 2018YFC0809002, and in part by the National Natural Science Foundation of China (NSFC) under Grant 51677093 and Grant 51777100.

ABSTRACT Lamb wave inspection provides a promising method to assess the structural health status. However, Lamb wave modes exhibit different characteristics which vary with frequency significantly. The best excitation frequency usually cannot be determined in specific applications. This work proposes a multifrequency exploitation and identification method. Lamb waves of multiple frequencies are excitated simultaneously to utilize diverse attributes of Lamb waves in different frequency ranges. This paper firstly analyzes the detectability and sensitivity of Lamb wave. Then the multifrequency exploitation scheme and corresponding post-processing method are introduced. Relevant simulations by finite element method are conducted to verify its effectiveness. Experiments of single-frequency and multifrequency excitations are implemented. The investigations indicate that the proposed method can avoid the missing of defects compared with single-frequency excitation. In addition, a post-processing method is suggested and the results demonstrate that the multifrequency excitation also provides high accuracy in defect location.

INDEX TERMS Finite element method, Lamb wave, multifrequency excitation, signal post-processing.

I. INTRODUCTION

The ultrasonic guided wave inspection has the potential of longer distance and higher effeciency than traditional structural health monitoring methods [1]–[4]. Lamb waves, one type of guided wave propagating in plate-like structure, have been utilized widely in material inspections [5], [6]. It can be generated by piezoelectric transducer or electromagnetic ultrasonic transducer (EMAT) [7], [8].

The Lamb wave signal contains information of the structural health status along the propagation path. Through extracting and interpreting the received Lamb wave signal, the location and quantification of defects, even the imaging of inspected structures can be accomplished. The information used to diagnose the structure includes time, amplitude and phase of the Lamb wave signal. The arrival time was extracted to detect corrosion in aluminum aircraft structural stringers [9]. The time of flight (TOF) and wave amplitude of received signal were considered as the input of wavelet network to estimate the damage location and severity [10]. Furthermore, tomographic imaging derived from medical research has been implemented in steel plate inspection using the TOF of Lamb waves [11].

Recently Lamb waves attracts considerable attention. However, the characteristics of Lamb waves vary with its frequency significantly. Frequency and mode selection are important considerations in Lamb wave inspection systems. For a specific application, the best excitation frequency is usually unknown. To find the appropriate frequency, a chirp signal was utilized to generate multiple frequencies of Lamb waves simultaneously and deconvolution was applied to extract narrowband responses. The responses were used as the reference in frequency selection and optimization [12]. Chirp excitation and pulse compression in communication field were introduced to filtr the received signal and improve the accuracy of defect location [13], [14]. Ridge tracking and time-varying filter were adopted to isolate interfered Lamb waves excitated by a chirp signal [15]. An alternative technique of squeezed wavelet transform was also studied to identify broadband Lamb waves generated by a triangle impulse [16]. Broadband excitation could provide more information than single-frequency tone-burst. However, the overlapped wavepackets of different frequencies bring complicated signal post-processing and interpretation.

The associate editor coordinating the review of this manuscript and approving it for publication was Zhaoqing Pan.

The broadband excitation scheme is difficult to be applied in real inspection and the excitation waveform needs more investigations.

Lamb waves exhibit frequency dispersion and multiple modes, which increase the difficulties of information extraction. Dispersion compensation has been developed to suppress the modal dispersion [17]. It was implemented in numerical method by transforming the time-domain signal into distance space. A simplified dispersion elimination algorithm has been accomplished by compensating the second-order nonlinear phase shift of the wave signal [18]. For the multimodal Lamb wave, two-dimensional Fourier transform was applied to identify and measure the amplitudes of multi-mode signals [19]. Time and frequency representation (TFR) also provides a promising tool to analyze non-stationary Lamb wave signals. The used TFRs include wavelet transform, chirplet transform, Wigner-Ville distribution (WVD) and so forth [20]–[24]. In case of multimodal dispersive Lamb wave signal, an effective post-processing method is still a challenge in the promotion of Lamb wave inspection.

To address the diverse features in specific applications and avoid the problem of undetected flaws when utilizing Lamb wave, a multifrequency exploitation scheme and corresponding signal processing method are proposed. In the work described here, the characteristic analysis of Lamb waves is conducted, especially the interaction of wave and defect. Then the process of a multifrequency excitation and identification method is provided. This method has been verified by relevant simulations and experiments. The comparison with single-frequency excitation proves that the proposed method has more accurate defect inspection.

The research is organized as follows. Section II presents the characteristic analysis of Lamb waves and the sensitivities of Lamb waves in different frequency ranges are discussed. In section III, the multifrequency exploitation scheme is proposed and its procedures are summarized in detail. The validation of the proposed method is conducted firstly by simulation analysis in Section IV. Section V implements experimental investigations and compares the multifrequency excitation with single-frequency excitation. Concluding remarks are given in Section VI.

II. CHARACTERISTIC ANALYSIS OF LAMB WAVE

Lamb wave is one type of elastic waves and its theory can be described by elastodynamics with conditions of free boundaries. Multiple modes exist in plate simultaneously and the illustration of Lamb wave is presented in Fig. 1. The symmetric and anti-symmetric modes are denoted as S and A modes. The theoretical expression for Lamb wave is well known as the Rayleigh-Lamb equation [5]:

$$S\ mode: \quad \frac{\tan(qh)}{\tan(ph)} = -\frac{4k^2pq}{(q^2-k^2)^2} \tag{1}$$

$$A\ mode: \quad \frac{\tan(qh)}{\tan(ph)} = -\frac{(q^2-k^2)^2}{4k^2pq} \tag{2}$$

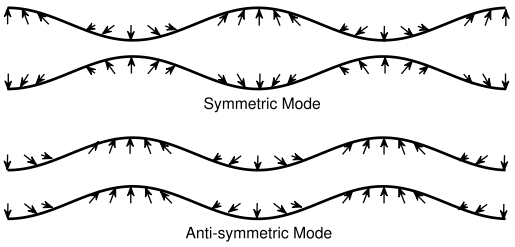

FIGURE 1. Illustration of symmetric and anti-symmetric lamb wave modes.

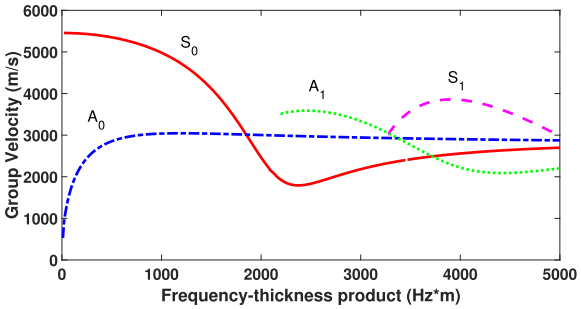

FIGURE 2. Dispersion curve of Lamb wave from numerical solution of Rayleigh-Lamb equation.

where, $h = d/2$, $p^2 = \omega^2/c_L^2 - k^2$, $q^2 = \omega^2/c_T^2 - k^2$, $k = \omega/c_p$. d is the plate thickness, ω is the angular frequency, c_L is the longitudinal wave velocity. c_T is the transverse wave velocity, k is the wave number and c_p is the phase velocity of Lamb wave.

Lamb waves have the potential to inspect the whole structure, not only the surface detection. It can be applied in pitch-catch or pulse-echo configuration. However, several factors are vital to consider before the defect inspection.

First, it is difficult to generate pure mono-frequency signal in real inspection. From Rayleigh-Lamb equation, the phase velocity of Lamb wave depends on the parameters of plate and excitation frequency. This phenomenon is called dispersion. Moreover, the group velocity c_g, which is the velocity of Lamb wavepacket, can be derived from phase velocity as $c_g = d\omega/dk$. Through solving the Rayleigh-Lamb equation numerically, the dispersion curve can be obtained as Fig. 2 shows. The velocity is regarded as the function of frequency-thickness product. Therefore, the actual wavepackets of not pure mono-frequency will extend in time duration due to dispersion. It might lead to the overlaps of received signals and bring negative influence on the interpretation of signals.

Second, different transducers have different excitability and detectability of Lamb waves. Piezoelectric transducer and EMAT are usually utilized to generate Lamb wave [3]. In the case of EMAT, it has the advantage of non-contact and can be applied under special environments such as high temperature. EMAT can be considered as transfer function which has individual frequency responses. The wave generation mechanism of omnidirectional EMAT had been modeled and the wavelength of Lamb wave was related to the

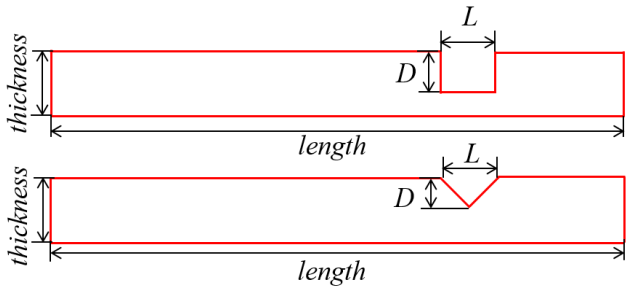

FIGURE 3. The shapes of rectangular defect and triangular defect.

TABLE 1. Type of defects and the parameters.

Defect Type	Defect Length (m)	Depth Ratio
Rectangular Defect	0.01	75%
Triangular Defect	0.01	75%

size of magnetostrictive patch [25]. The generated Lamb wave modes could also be optimized by shaping magnetic field [26].

Third, the sensitivity to defects varies for Lamb waves of different frequencies and modes [27]. For the sake of simplicity, only the fundamental symmetric mode (S_0) is studied by analyzing the reflection coefficient (RC) of Lamb wave when it encounters defects. To investigate the relation between RC and frequency, the finite element method (FEM) is used to simulate the behavior of Lamb wave. The ABAQUS package is adopted to implement the FEM. A Python script is written to execute repetitive tasks conveniently.

Lamb wave can be modeled as plane-strain problem and the 2D model is established. Two types of defects are considered: rectangular slot and triangular slot which are shown in Fig. 3. The defect length is marked as L. The defect depth is expressed as the percentage of plate thickness and marked as D. The parameters are shown in Table 1. The thickness and length of the plate is 4 mm and 1 m, respectively. The plate is modeled as steel material with Young's modulus of 207 GPa, Poisson's ratio of 0.3 and density of 7800 k_g/m^3. The single-frequency tone-burst is used as the excitation signal imposed on the plate. The tone-burst is 5-cycle sinusoidal signal with Hamming window.

Through changing the frequency and repeating the simulations, the direct wave and reflected wave at the inspecting point are obtained. RC is expressed as the ratio of their amplitudes

$$RC = \frac{A_r}{A_d} \tag{3}$$

where A_r and A_d are the amplitude of direct wave and reflected wave. The results for S_0 mode are presented in Fig. 4. It clearly shows that the reflection coefficients of Lamb wave encountering with two defects present their

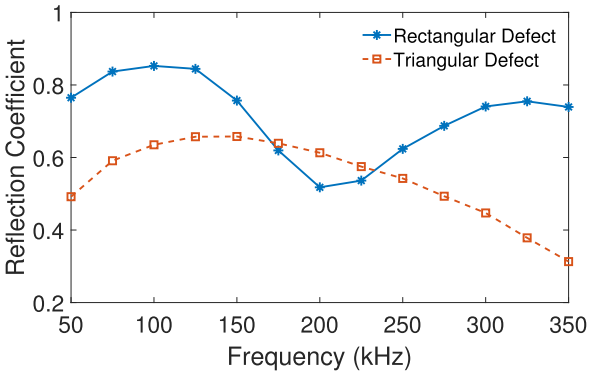

FIGURE 4. Reflection coefficients of different frequencies for S_0 mode.

distinctive features. For the rectangular defect, two peaks of RC appear at 100 kHz and 325 kHz and one valley appears at 200 kHz. The difference between the maximum and minimum RC is approximately 0.35. If the inspection system utilizes the reflected wave, the larger the wave amplitude, the more probability the defect is detected. In the case of triangular defect, the RC curve is nearly parabolic and one peak appears at 150 kHz. The actual defect shape is more complicated because of the corrosion and stress condition. Therefore, the defect will present unknown RC features.

The attenuation characteristic is another factor. Different frequencies of Lamb waves face different attenuations by the material of the inspected structure [28]. The attenuation will reduce the amplitude of Lamb wave and decrease the propagation distance. In conclusion, due to the diverse characteristics of Lamb wave, the frequency and mode need to be selected deliberately to acquire better inspection effect.

III. PROPOSED MULTIFREQUENCY EXPLOITATION METHOD

In actual industrial inspection, the potential defect types in structure and model of transducer are difficult to obtain. The prior knowledge of detectability and sensitivity of Lamb wave is usually unknown. To overcome the complicated Lamb wave frequency decision, the method of multifrequency exploitation and identification is proposed. The block diagram of the algorithm is shown in Fig. 5. The details are described in following parts.

A. SCHEME OF MULTIFREQUENCY EXCITATION

According to the dispersion equation, infinite modes of Lamb waves might exist in a plate. Different modes exhibit different wave structures and present unique sensibility towards various defects. However, it is difficult to interpret the information under multiple Lamb wave modes. To avoid the negative effect of multimodes, the multiple frequencies of fundamental modes (A_0 and S_0) are selected.

The higher modes of Lamb waves have a lowest excitation frequency called cutoff frequency f_c. For the steel plate with the parameters given above for the simulation, the cutoff frequency of S_1 and A_1 mode is 400 kHz which can be obtained

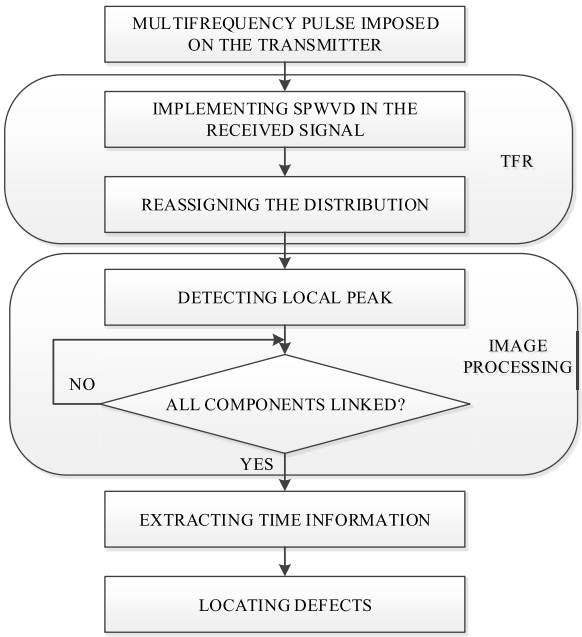

FIGURE 5. Scheme diagram of the multifrequency exploitation algorithm. SPWVD is the smoothed-pseudo Wigner-Ville distribution and TFR is the time and frequency representation.

TABLE 2. The group velocities of selected lamb waves.

Frequency (kHz)	Group Velocity of S_0 (m/s)	Group Velocity of A_0 (m/s)
100	5372.50	2812.75
200	5276.54	3140.02
300	5061.65	3213.29

from the dispersion equation. To utilize the advantage of multifrequency excitation, the frequencies are chosen evenly from 0 to f_c. In the following analysis, three frequencies of Lamb waves are excitated to inspect the plate structure. The expression of excitation pulse is given by

$$S_{mf}(t) = w(t) \cdot [sin(2\pi f_1\, t) + sin(2\pi f_2\, t) + sin(2\pi f_3 t)] \quad (4)$$

where $w(t)$ is the added window function, f_1, f_2, f_3 are 100, 200 and 300 kHz respectively. The Hamming function is selected as the window and it can be expressed as

$$w(t) = 0.54 - 0.46 \cdot cos(2\pi t/T) \quad (5)$$

where T is the time duration of the pulse. The use of window function can help reduce the spectrum leakage caused by truncation effect. Under the three excitation frequencies, the group velocities are calculated and compiled in Table 2.

The multifrequency signal is imposed on the transmitter. When Lamb waves encounter defects, the transmission and reflection of waves both occur after the interaction. Then the receiver placed in a certain distance from the transmitter detects the reflected signal. By extracting the information in reflected Lamb wave, the location, even the shape of defect can be determined.

B. HIGH RESOLUTION TFR AND ITS REASSIGNMENT

To interpret the information in signal, combination of TFR reassignment with multicomponents extraction is proposed.

Through adding the time window, short time Fourier transform (STFT) introduces the time-frequency plane. Furthermore, joint time-frequency analysis is developed and WVD is given as follows:

$$W_x(t,f) = \int x(t+\frac{\tau}{2})x^*(t-\frac{\tau}{2})e^{-j2\pi f\tau}d\tau. \quad (6)$$

where '$*$' denotes conjugate operation and τ is the time-shift. For mono-component linear frequency modulation signal, WVD presents better time-frequency concentration than other distributions. For multiple components, cross-terms are generated which weaken the identification of auto-terms. To reduce the cross-terms, smoothing functions in both time and frequency domains are imposed on WVD. And these two functions are independent so that the time and frequency resolution can be improved separately. The modified distribution is known as smoothed-pseudo-WVD (SPWVD) [29]. It is expressed as

$$SPW_x(t,f;G) = \int\int W_x(u,\xi)G(t-u,f-\xi)dud\xi \quad (7)$$

where u is the time-shift, ξ is the frequency-shift and $G(t,f)$ is the two-dimensional Fourier transform of smoothing window which allows the independent control of smoothing in time and frequency domain. To increase the readability of TFR, time-frequency reassignment method provides a powerful tool to concentrate the energy and reduces the interference terms [30]. The key point of the reassignment principle is to move the average of energy around (t,f) from the geometrical center to gravity center of the local domain. The process is expressed by

$$\hat{t}(x;t,f) = \frac{\int uG(t-u,f-\xi)W_x(u,\xi)dud\xi}{\int G(t-u,f-\xi)W_x(u,\xi)dud\xi} \quad (8)$$

$$\hat{f}(x;t,f) = \frac{\int \xi G(t-u,f-\xi)W_x(u,\xi)dud\xi}{\int G(t-u,f-\xi)W_x(u,\xi)dud\xi}. \quad (9)$$

Then the reassigned SPWVD (RSPWVD) is

$$RSPW_x(t',f';G) = \int\int SPW_x(t,f;G)\,\delta(t'-\hat{t}(x;t,f))\delta(f'-\hat{f}(x;t,f))dtdf \quad (10)$$

where δ is the Dirac delta function. The reassigned distribution can help increase the concentration of the signal components and represent higher resolution.

C. MULTIPLE COMPONENTS SEPARATION

To obtain the accurate TOF, components separation and extraction are accomplished by applying image processing technology.

The local peak value in RSPWVD is firstly extracted. The peak points satisfy two conditions, namely, the first-order partial derivative with respect to frequency is equal to zero while the second-order partial derivative is negative. It can be expressed as

$$RSPW_x(t,f)_{peak}: \left\{\frac{\partial\, RSPW_x(t,f)}{\partial f}=0\right\} \text{ and } \left\{\frac{\partial^2 RSPW_x(t,f)}{\partial f^2}<0\right\}. \quad (11)$$

Like the pixels connection in images, the discrete peak points are linked to form individual components based on the local peak detection [31]. After the component extraction by the linking algorithm, the features of each component can be analyzed.

D. TOF EXTRACTION AND DEFECT LOCATION DETERMINATION

The linked component in time-frequency domain represents the frequency at specific time. The instantaneous frequency (IF) originated from communication field is introduced to describe this linked curve. By finding the time corresponding to the excitation frequency in the IF curve, the TOF can be determined. If the TOFs of direct wave and reflected wave are t_1 and t_2 respectively, then the distance between the receiver and defect can be calculated as

$$d=\frac{t_2-t_1}{2}\cdot c_g \quad (12)$$

where c_g is the group velocity of Lamb wave. It is noticed that c_g is not constant and it can be derived from dispersion curve according to the frequency.

IV. SIMULATION ANALYSIS

To validate the effectiveness of the proposed multifrequency excitation method, simulation analysis is conducted based on ABAQUS. The 2D model is adopted and the finite element is CPE4R, which is one type of two-dimensional solid element. The size of elements Δx is an important parameter to ensure the accuracy of simulation results. In the case of acoustic wave, the element size should be much smaller than the wavelength λ. Usually, it follows the principle below:

$$\Delta x \le \frac{\lambda}{N} \quad (13)$$

where N should be larger than 10 in general. To observe the propagation of Lamb waves, the time transient analysis is applied. The time step Δt in the simulation is selected as

$$\Delta t \le \frac{\Delta x}{c} \quad (14)$$

where c is the speed of longitudinal wave.

Single rectangular defect with length of 0.015 m and depth ratio of 75 % is considered in the simulation. The multifrequency pulse is loaded at the left boundary of the plate. The inspection point is located between the excitation point and defect. The defect is 4.0 m away from excitation point and 2.0 m away from inspection point. The displacement captured at 278.68 μs in the simulation is depicted in Fig 6. Two modes appear simultaneously and the right wavepacket is faster than the left wavepacket. The left and right waves are S_0 and A_0 mode respectively. The distance between two modes is consistent with the theoretical value calculated from the velocity and propagating time.

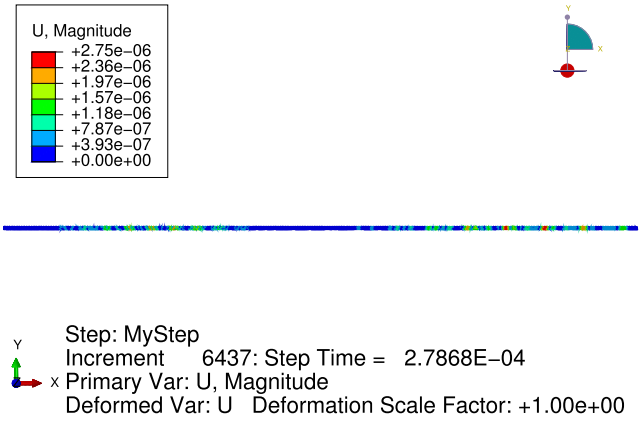

FIGURE 6. The displacement captured at 278.68 μs in the simulation.

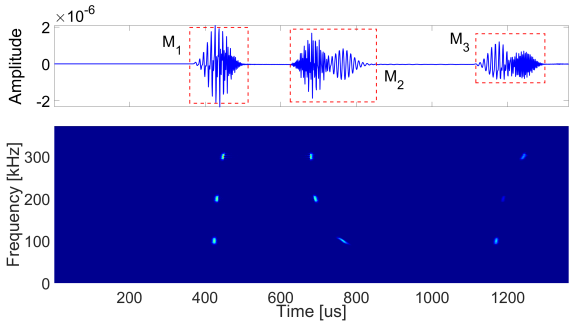

FIGURE 7. The multifrequency signal from the simulations and its reassigned distribution.

The received signal and its reassigned time-frequency distribution using proposed signal processing method are shown in Fig. 7. The wavepackets of M_1 and M_2 are direct S_0 and A_0 mode respectively. M_3 is the reflected S_0 mode after the interaction of direct wave and rectangular defect. The overlapped wavepackets are separated distinctly in the time-frequency domain and the components are perfectly concentrated. It demonstrates that the proposed method is capable of distinguishing multifrequency Lamb wave. The brighter color means the larger energy. It indicates that reflected wave of 200 kHz owns the lowest energy, which is consistent with the RC relation in above analysis.

Then the individual components are extracted and the IF curves are shown in Fig. 8. According to the IF curve, the TOF of corresponding frequency is found. In the case of 100 kHz, the TOFs of direct wave and reflected wave are 0.419 and 1.174 ms respectively. The group velocity of Lamb wave in 100 kHz is 5372.5 m/s. Using (12), the distance of defect

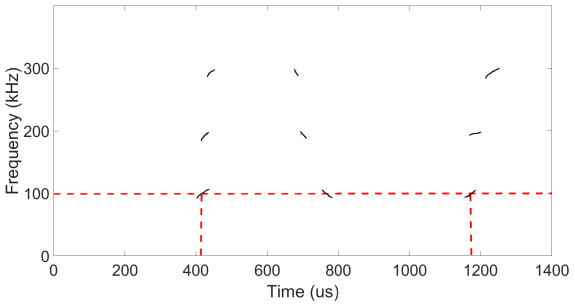

FIGURE 8. Extracted components and IF curves from the time-frequency reassignment.

and receiver is 2.028 m. The calculated distance is in accord with the actual value 2 m. The relative error can be calculated by (15) and the result is 1.5%. It proves that the proposed method can also accurately locate the defect.

$$Relative\ error = \left| \frac{d_{cal} - d_{ac}}{d_{ac}} \right| \cdot 100\% \tag{15}$$

where d_{cal} is the calculated distance by the proposed method and d_{ac} is the actual value.

V. EXPERIMENTAL STUDY AND DISCUSSION

A. EXPERIMENTAL SETUP

The Lamb wave inspection system is established on the 4 mm thick steel specimen. The EMAT, composed of coil and magnet is used as Lamb wave transmitter and receiver. Photographs of the EMAT are provided in Fig. 9(a). To avoid the boundary reflection, the transmitter is placed far away from the left boundary of plate. The receiver is set 3 m away from transmitter. The multifrequency pulse is produced by arbitrary waveform generator and then amplified by high power pulser. The detected signal from receiver is amplified and filtered by signal conditioning circuit. The data is collected to computer by Data Acquisition (DAQ) System. Finally the data is post-processed by the proposed method which is coded in MATLAB.

Two types of slots have been machined in the steel specimen: a rectangular defect and a triangular defect. The two defects are located between the receiver and the right boundary of plate. The schematic diagram is depicted in Fig. 9(b). The triangular defect is closer to the receiver than the rectangular defect. The distances between the defects and receiver are 2 m and 5 m respectively. The purpose of this designed experiment is to verify the advantage of identifying two defects when using multifrequency excitation.

B. SINGLE-FREQUENCY EXCITATION SCHEME

Single-frequency excitation signal is firstly loaded to the transmitter. The frequency of 200 kHz is selected to employ the experiment. The received signal and the extracted IF curves are presented in Fig. 10.

Several wavepackets appear in Fig. 10(a). The fastest wavepacket P_0 is the electromagnetic induction signal which

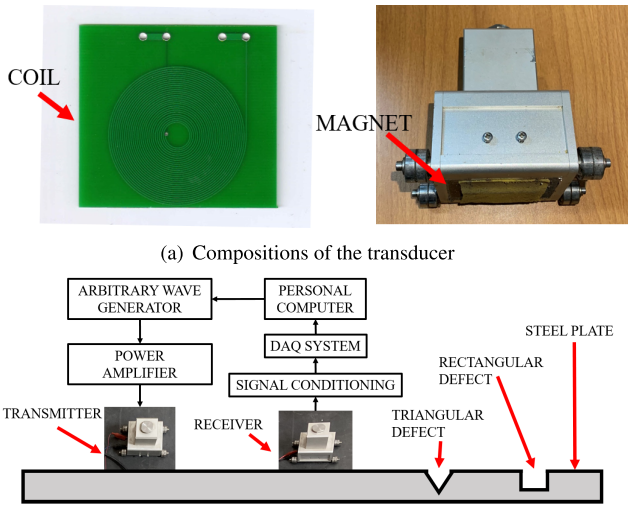

(a) Compositions of the transducer

(b) Illustration of Lamb wave experimental system

FIGURE 9. Schematics of lamb wave experimental setup.

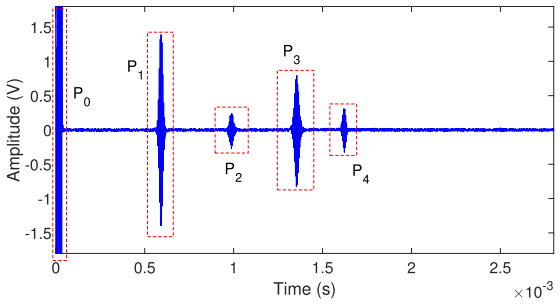

(a) The received signal in single-frequency excitation experiments

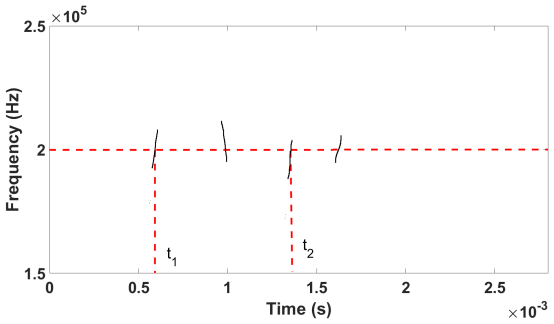

(b) The extracted individual components

FIGURE 10. Results of single-frequency excitation experiments.

has high amplitude. According to the group velocity and the propagation distance, the middle two wavepackets P_1 and P_2 are the direct waves which propagate from the transmitter to receiver directly. They are S_0 and A_0 mode respectively. The wavepacket of P_3 is reflected S_0 wave from triangular defect, while P_4 is A_0 mode which is generated by mode conversion occurred in the interaction of Lamb wave with defect. After the post-processing of the received signal (P_0 is omitted), the result is shown in Fig. 10(b). The TOF is easily read from the IF curve. Since S_0 mode has the larger amplitude than A_0 mode, S_0 mode is utilized to locate

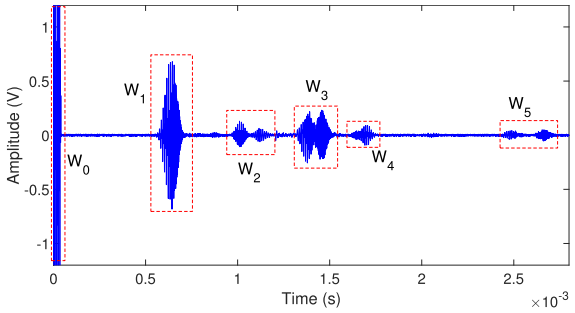

FIGURE 11. The received signal in multifrequency excitation experiments.

the defect. The TOFs of direct wave and reflected wave are 0.584 and 1.354 ms respectively. Then location of triangular defect is 2.032 m and the relative error is 1.6 %.

Although noise is unavoidable problem in Lamb wave signal, it has been reduced significantly by multiple repeated experiments and average processing. In this case, the number of repetitions is 10 and the noise is rather small in the received signal. However, no apparent reflected wave from the rectangular defect is received. The rectangular defect is set in the right of triangular defect and the direct wave encounters with triangular defect firstly. In the interaction of Lamb wave with triangular defect, a certain proportion of energy is reflected back while the other continues to propagate forward. The damping effect of steel material also causes the energy loss in Lamb wave. When the transmitted wave encounters with the rectangular defect, rather small energy is reflected back due to the low RC in case of Lamb wave in 200 kHz. With the attenuation in the propagation path, the reflected wave from rectangular defect is difficult to detect by the receiver. Therefore, only the triangular defect is detected, while the rectangular defect is missed out.

As Fig. 10(a) shows, the received signal of single-frequency excitation is simple. Although the wave signal is extended in time domain due to the dispersion phenomenon, the waveform is separated apparently and easy to be analyzed compared with the waveform of multifrequency signal presented in Fig. 7. In case of single-frequency excitation scheme, the wavepackets are clear to be recognized. However, if the frequency is not suitable in the specific application, some flaws might not be detected and this error would influence the evaluation of plate structure.

C. MULTIFREQUENCY EXPLOITATION SCHEME

Three different frequencies below the cutoff frequency are chosen in this study. To utilize the advantage of different frequencies, the selected frequencies are evenly distributed from zero to cutoff frequency. Thus, the 100, 200 and 300 kHz are superposed as the multifrequency excitation signal. The results of this experiment are presented in Fig. 11.

Similar with the single-frequency excitation, several wavepackets appear in time domain. Due to the multiple frequencies coexisting in the signal and the inherent dispersion phenomenon, the wavepackets are extended with longer time duration and wavepackets of different frequencies are

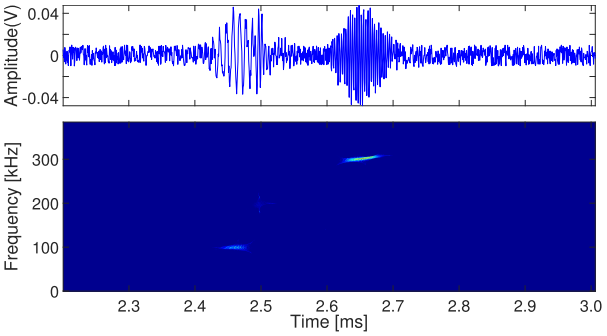

FIGURE 12. The wavepacket W_5 and its reassigned distribution.

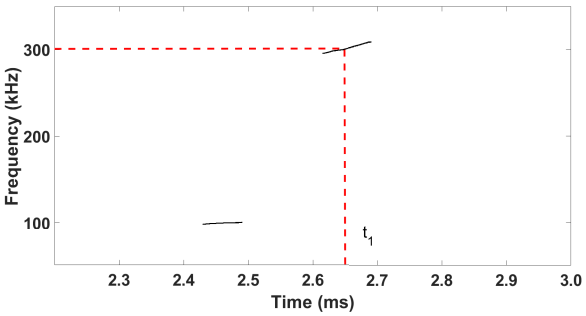

FIGURE 13. The extracted individual components from wavepacket W_5.

overlapped in time domain. The multifrequency Lamb waves in same mode are not separated because the gap of their velocities are rather small. The fastest wavepacket W_0 is the electromagnetic induction signal. The wavepackets W_1 and W_2 are the direct waves of S_0 and A_0 mode respectively. W_3 is the reflected S_0 mode. W_4 is the A_0 mode generated from the mode conversion in the interaction between direct S_0 mode and triangular defect. W_5 is the reflected wave from rectangular defect. Although the amplitude is small, it is still enable to be detected.

To describe the signal clearly, the reassigned time-frequency distribution is applied and the results of wavepacket W_5 are presented in Fig. 12. As the TFR shows, this method distinguishes the individual components without any confusion. After the post-processing of the time-frequency reassignment, corresponding IF curves are extracted and the results are shown in Fig. 13.

Since the energy of 300 kHz is considerably larger than that of 100 and 200 kHz, this frequency of 300 kHz is utilized to calculate the TOF and defect location. The direct wave, reflected wave from triangular defect and from rectangular defect are 0.644, 1.455 and 2.659 ms, respectively. The calculated distance and relative error are presented in Table 3. The location error of triangular defect and rectangular defect are 2.63 % and 2.0 % respectively. The results indicate that the proposed method provides high accurate defect location.

Comparing the results of multifrequency excitation with that of the single-frequency, the received signal of the former is more complicated. Lamb waves of multiple frequencies propagate at different velocities. The wavepackets after a

TABLE 3. Defects location and relative error.

Defect Type	Calculated Value (m)	Actual Value (m)	Relative Error
Triangular Defect	2.053	2.0	2.63%
Rectangular Defect	5.10	5.0	2.0%

shorter transmission distance will be overlapped, while after a longer distance, the space gap of wavepackets are widened and more wavepackets appear. This increases the recognition of different Lamb waves in time domain. Through the high resolution of time-frequency reassignment, the wavepackets are separated clearly in two-dimensional plane and then the features are enable to be extracted. The location errors of multifrequency excitation are a bit larger than that of the single-frequency, but the differences are not significant and the errors are in the same order of magnitude. Multifrequency excitation takes advantage of diverse attributes of Lamb waves in different frequencies, accordingly it also brings the difficulties in post-processing of received signal.

VI. CONCLUSION

In this work, a novel method of multifrequency exploitation and identification is proposed aimed at detecting all defects simultaneously in Lamb wave inspection. The best excitation frequency of Lamb wave is nearly impossible to determine in certain applications due to the complicated relation between the detection sensitivity and frequency of Lamb wave. The multifrequency excitation permits the effective inspection using Lamb wave of multiple frequencies. The simulation applying Lamb wave to detect the rectangular defect verifies the availability of multifrequency exploitation scheme. Moreover, the experimental investigations indicate that two flaws are detected through applying multifrequency excitation, while only one defect in single-frequency excitation. Although the multifrequency excitation causes more wavepackets and overlapped waveform in time domain, the time-frequency reassignment presents high resolution in two-dimensional plane. In addition, the extracted time information from the post-processing method provides high accuracy in defect location. Therefore, the proposed multifrequency exploitation method can act as an efficient approach for Lamb wave inspection. Future research will analyze this method in the application of defect quantification and further imaging.

REFERENCES

[1] J. L. Rose, "Guided wave nuances for ultrasonic nondestructive evaluation," *IEEE Trans. Ultrason., Ferroelectr., Freq. Control*, vol. 47, no. 3, pp. 575–583, May 2000.
[2] M. Mitra and S. Gopalakrishnan, "Guided wave based structural health monitoring: A review," *Smart Mater. Struct.*, vol. 25, no. 5, 2016, Art. no. 053001.
[3] R. Guan, Y. Lu, W. Duan, and X. Wang, "Guided waves for damage identification in pipeline structures: A review," *Struct. Control Health Monitor.*, vol. 24, no. 11, 2017, Art. no. e2007.
[4] L. Zeng, L. Huang, and J. Lin, "Damage imaging of composite structures using multipath scattering Lamb waves," *Compos. Struct.*, vol. 216, pp. 331–339, May 2019.
[5] J. L. Rose, *Ultrasonic Guided Waves in Solid Media*. Cambridge, U.K.: Cambridge Univ. Press, 2014.
[6] S. Wang, S. Huang, Q. Wang, Z. Wang, and W. Zhao, "Characterizing excitability of Lamb waves generated by electromagnetic acoustic transducers with coupled frequency domain models," *Ultrasonics*, vol. 93, pp. 71–80, Mar. 2019.
[7] A. Raghavan and C. E. S. Cesnik, "Finite-dimensional piezoelectric transducer modeling for guided wave based structural health monitoring," *Smart Mater. Struct.*, vol. 14, no. 6, p. 1448, 2005.
[8] S. Wang, S. Huang, Y. Zhang, and W. Zhao, "Modeling of an omnidirectional electromagnetic acoustic transducer driven by the Lorentz force mechanism," *Smart Mater. Struct.*, vol. 25, no. 12, 2016, Art. no. 125029.
[9] J. Bingham and M. Hinders, "Lamb wave characterization of corrosion-thinning in aircraft stringers: Experiment and three-dimensional simulation," *J. Acoust. Soc. Amer.*, vol. 126, no. 1, pp. 103–113, 2009.
[10] H. Z. Hosseinabadi, B. Nazari, R. Amirfattahi, H. R. Mirdamadi, and A. R. Sadri, "Wavelet network approach for structural damage identification using guided ultrasonic waves," *IEEE Trans. Instrum. Meas.*, vol. 63, no. 7, pp. 1680–1692, Jul. 2014.
[11] Z. Wei, S. Huang, S. Wang, and W. Zhao, "Magnetostriction-based omnidirectional guided wave transducer for high-accuracy tomography of steel plate defects," *IEEE Sensors J.*, vol. 15, no. 11, pp. 6549–6558, Nov. 2015.
[12] J. E. Michaels, S. J. Lee, A. J. Croxford, and P. D. Wilcox, "Chirp excitation of ultrasonic guided waves," *Ultrasonics*, vol. 53, no. 1, pp. 265–270, 2013.
[13] L. De Marchi, A. Perelli, and A. Marzani, "A signal processing approach to exploit chirp excitation in Lamb wave defect detection and localization procedures," *Mech. Syst. Signal Process.*, vol. 39, nos. 1–2, pp. 20–31, 2013.
[14] D. Zhang, Z. Zhou, J. Sun, E. Zhang, Y. Yang, and M. Zhao, "A magnetostrictive guided-wave nondestructive testing method with multifrequency excitation pulse signal," *IEEE Trans. Instrum. Meas.*, vol. 63, no. 12, pp. 3058–3066, Dec. 2014.
[15] M. Zhao, L. Zeng, J. Lin, and W. Wu, "Mode identification and extraction of broadband ultrasonic guided waves," *Meas. Sci. Technol.*, vol. 25, no. 11, 2014, Art. no. 115005.
[16] S. Wang, S. Huang, Q. Wang, Y. Zhang, and W. Zhao, "Mode identification of broadband Lamb wave signal with squeezed wavelet transform," *Appl. Acoust.*, vol. 125, pp. 91–101, Oct. 2017.
[17] P. D. Wilcox, "A rapid signal processing technique to remove the effect of dispersion from guided wave signals," *IEEE Trans. Ultrason., Ferroelectr., Freq. Control*, vol. 50, no. 4, pp. 419–427, Apr. 2003.
[18] W. Wu and Y. Wang, "A simplified dispersion compensation algorithm for the interpretation of guided wave signals," *J. Pressure Vessel Technol.*, vol. 141, no. 2, 2019, Art. no. 021204.
[19] D. Alleyne and P. Cawley, "A two-dimensional Fourier transform method for the measurement of propagating multimode signals," *J. Acoust. Soc. Amer.*, vol. 89, no. 3, pp. 1159–1168, May 1990.
[20] W. H. Prosser, M. D. Seale, and B. T. Smith, "Time-frequency analysis of the dispersion of Lamb modes," *J. Acoust. Soc. Amer.*, vol. 105, no. 5, pp. 2669–2676, 1999.
[21] S. Legendre, D. Massicotte, J. Goyette, and T. K. Bose, "Wavelet-transform-based method of analysis for Lamb-wave ultrasonic NDE signals," *IEEE Trans. Instrum. Meas.*, vol. 49, no. 3, pp. 524–530, Jun. 2000.
[22] H. Kuttig, M. Niethammer, S. Hurlebaus, and L. J. Jacobs, "Model-based analysis of dispersion curves using chirplets," *J. Acoust. Soc. Amer.*, vol. 119, no. 4, pp. 2122–2130, 2006.
[23] C.-Y. Kim and K.-J. Park, "Mode separation and characterization of torsional guided wave signals reflected from defects using chirplet transform," *NDT E Int.*, vol. 74, pp. 15–23, Sep. 2015.
[24] D. Dai and Q. He, "Structure damage localization with ultrasonic guided waves based on a time–frequency method," *Signal Process.*, vol. 96, pp. 21–28, Mar. 2014.
[25] J. K. Lee, H. W. Kim, and Y. Y. Kim, "Omnidirectional Lamb waves by axisymmetrically-configured magnetostrictive patch transducer," *IEEE Trans. Ultrason., Ferroelectr., Freq. Control*, vol. 60, no. 9, pp. 1928–1934, Sep. 2013.
[26] P. B. Nagy, S. Francesco, and I. Geir, "Corrosion and erosion monitoring in plates and pipes using constant group velocity Lamb wave inspection," *Ultrasonics*, vol. 54, no. 7, pp. 1832–1841, 2014.
[27] M. J. S. Lowe and O. Diligent, "Low-frequency reflection characteristics of the s_0 Lamb wave from a rectangular notch in a plate," *J. Acoust. Soc. Amer.*, vol. 111, no. 1, pp. 64–74, 2002.

[28] P. Huthwaite, R. Ribichini, P. Cawley, and M. J. S. Lowe, "Mode selection for corrosion detection in pipes and vessels via guided wave tomography," *IEEE Trans. Ultrason., Ferroelectr., Freq. Control*, vol. 60, no. 6, pp. 1165–1177, Jun. 2013.
[29] F. Auger and P. Flandrin, "Improving the readability of time-frequency and time-scale representations by the reassignment method," *IEEE Trans. Signal Process.*, vol. 43, no. 5, pp. 1068–1089, May 1995.
[30] P. Flandrin, F. Auger, and E. Chassande-Mottin, "Time-frequency reassignment: From principles to algorithms," *Appl. Time-Freq. Signal Process.*, vol. 5, nos. 179–203, p. 102, 2003.
[31] L. Rankine, M. Mesbah, and B. Boashash, "IF estimation for multicomponent signals using image processing techniques in the time-frequency domain," *Signal Process.*, vol. 87, no. 6, pp. 1234–1250, Jun. 2007.

ZHE WANG received the B.S. degree from the School of Electrical Engineering, Chongqing University, Chongqing, China, in 2016. He is currently pursuing the Ph.D. degree with the Department of Electrical Engineering, Tsinghua University, Beijing, China.

His current research interests include electromagnetic measurement and nondestructive evaluation.

SONGLING HUANG received the bachelor's degree in automatic control engineering from Southeast University, Nanjing, China, in 1991, and the Ph.D. degree in nuclear application technology from Tsinghua University, Beijing, China, in 2001.

He is currently a Professor with the Department of Electrical Engineering, Tsinghua University. His research interests include nondestructive evaluation and instrument techniques.

SHEN WANG received the bachelor's and Ph.D. degrees in electrical engineering from Tsinghua University, Beijing, China, in 2002 and 2008, respectively.

He is currently an Associate Professor with the Department of Electrical Engineering, Tsinghua University. His research interests include nondestructive testing and evaluation, and virtual instrumentation.

QING WANG received the B.Eng. degree in electronic instrument and measurement technique from Beihang University, Beijing, China, in 1995, the M.Sc. degree in advanced manufacturing and materials from the University of Hull, Hull, U.K., in 1998, and the Ph.D. degree in manufacturing management from De Montfort University, Leicester, U.K., in 2001.

She is currently an Associate Professor with the Department of Engineering, Durham University, Durham, U.K. Her research interests include electronic instruments and measurement, computer simulation, and advanced manufacturing technology.

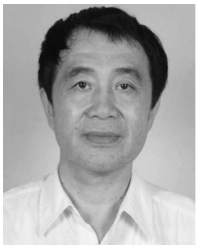

WEI ZHAO received the bachelor's degree in electrical engineering from Tsinghua University, Beijing, China, in 1982, and the Ph.D. degree from the Moscow Power Engineering Institute Technical University, Moscow, Russia, in 1991.

He is currently a Professor with the Department of Electrical Engineering, Tsinghua University. His research interests include modern electromagnetic measurement and instrument techniques.